Strain Effect Study on Mode Field Diameter and Effective Area of WII Type Single Mode Optical Fiber

Somayeh Makouei[1*], Fatemeh Makouei[1]

[1]Faculty of Electrical and Computer Engineering, University of Tabriz, Tabriz 51664, Iran
*corresponding author, E-mail: makouei@tabrizu.ac.ir

Abstract

In this article, the effect of strain on mode field diameter (MFD) and effective area (A_{eff}) in a modern multilayer WII type single mode optical fiber is investigated. The modal analysis of the fiber structure is based on linear polarized (LP) approximation method. The simulation results depict that both mode field diameter and effective area grow as a result of increment in tensile strain. The overall effect is observed in a slight rise in quality factor (Q_f) of the fiber. Likewise, enlargement in amplitude of compressive strain leads to decrement in MFD and A_{eff}. However, among the optical and geometrical parameters of the fiber structure, Δ has the most considerable impact on both MFD and A_{eff} variation whilst R_1 shows the least effect. In other words, any shift in the value allocated to Δ results in substantial change in the MFD and A_{eff} alteration due to strain. To eliminate this effect, the higher amounts for Δ are preferable which is related to the layering structure of the WII type optical fiber.

1. Introduction

Optical Fibers have revolutionized the telecommunications industry and have played a major role in the advent of the information age. The light, forming an electromagnetic carrier wave, is modulated to carry information through optical fiber. Fiber optic communications permit transmission over longer distances and at higher bandwidths (data rates). Due to low loss property in specified wavelengths and manageable dispersion developed efficiently, these fibers have attracted a great deal of interest. Recently, the multi-channel optical communication systems such as optical time division multiplexing (OTDM) and dense wavelength division multiplexing (DWDM) systems are requested for high capacity information communication [1]. Development of optical fibers with appropriate properties to meet multi-channel communication demands is of great importance. Multi-mode fibers generally have a wider core diameter and are used for short-distance communication links and for applications where high power must be transmitted. The data transmission in different modes contributes to the dispersive nature of optical fiber negatively and results in inter-modal cross talk. This effect limits modulation bandwidth and therefore data transmission capacity of optical fiber link. In order to restrict inter-modal cross talk effect in all long distance telecommunications, the single mode (SM) propagation is needed [2]. A suitable optical fiber should hold a small pulse broadening factor (small dispersion and dispersion slope), as well as small nonlinearity (large effective area) and low bending loss (small mode field diameter) for long distance transmission, especially when repeaters cannot be used [3]. The fiber loss, leading to distortions in the pulse shape and reductions in the pulse amplitude, restricts the maximum distance that information can be sent without presence of the repeaters. The performance of a designed structure may be assessed in terms of the quality factor. This dimensionless factor determines the trade-off between mode field diameter, which is an indicator of bending loss and effective area, which provides a measure of signal distortion owing to nonlinearity [4]. For a designed channel, the environmental perturbations actively impress the channel performance. Therefore, another important concept to consider is the impact of environmental factors such as humidity, temperature, strain, etc. on fiber properties.

A triple-clad fiber was firstly studied by Cozens and Boucouvalas as an optical coupler for sensing [5]. Triple-clad single-mode fibers have gained significant attention because of their perfect transmission properties that can be achieved by adjusting the multi-parameters [6-8]. Among the environmental interferences, the effect of temperature variation on multilayer fibers have been previously investigated by Rostami and Makouei [9]. Also, a proposal for the multiclad optical fiber structure with ultralarge effective area and small bending loss is presented [3]. Rostami and Oskouei [10, 11] have presented the analytical research about dispersion behavior of multi-clad fibers. In another report the effective area increment impact on dispersion property of R-type fibers is discussed [12]. The work reported in this article studies the dependence of the MFD and effective area of the WII-type single mode optical

fiber on environmental factor of strain. Application of force or strain to optical fiber during the installation process or any other possible reason and, leads to the variation in the refractive index of the fiber, and hence determinative factors of MFD and A_{eff} which stand for fiber loss property and fiber resistivity to nonlinear effects. In this work the multi-clad fiber is analyzed using the weakly guiding approximation (LP) [13]. This approximation is justified by the fact that all the materials used in the fiber fabrication have small refractive index differences.

This paper is organized as follows. In section 2 materials and methods are presented which cover the LP approximation and background formulation for the strain effect on the refractive index. Simulation results and discussions are presented in section 3. Finally, the paper ends with the brief conclusion.

2. Materials and Methods

In this section, we present modal analysis based on linearly polarized approximation (LP) for the WII type triple clad single mode optical fiber illustrated in Figure 1 [13]. This LP mode dispersion equation contains the radial mode number, which relates the electric field to the fiber radius and the azimuthal mode number exhibiting the angular dependence of the electrical field [2].

For this structure the index of refraction is defined as follows.

$$n(r)=\begin{cases} n_1, & 0<r<a, \\ n_2, & a<r<b, \\ n_3, & b<r<c, \\ n_4, & c<r, \end{cases} \tag{1}$$

where r is the radius position of the optical fiber. The effective refractive index is given by

$$n_{eff}=\frac{\beta_g}{k_0}, \tag{2}$$

where β_g is the longitudinal propagation constant of the guided mode and k_0 is the wave number in vacuum.

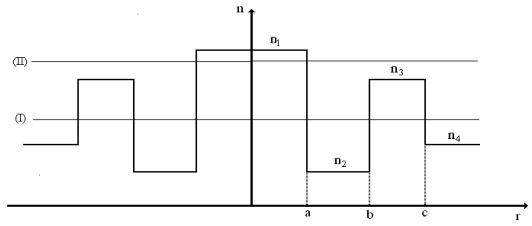

Figure 1. The index of refraction profile for the proposed structures (WII).

According to LP approximation to calculate the electrical field distribution, there are two regions of operation and the guided modes and propagating wave vectors can be obtained by using two determinants which are constructed by boundary conditions [13]. The two lines drown in Figure 1 demonstrate these two operation regions.

$$\begin{vmatrix} J_v(\kappa_1 a) & -I_v(\gamma_2 a) & -K_v(\gamma_2 a) & 0 & 0 & 0 \\ 0 & I_v(\gamma_2 b) & K_v(\gamma_2 b) & -J_v(\kappa_3 b) & -Y_v(\kappa_3 b) & 0 \\ 0 & 0 & 0 & J_v(\kappa_3 c) & Y_v(\kappa_3 c) & -K_v(\gamma_4 c) \\ \kappa_1 a J_v'(\kappa_1 a) & -\gamma_2 a I_v'(\gamma_2 a) & -\gamma_2 a K_v'(\gamma_2 a) & 0 & 0 & 0 \\ 0 & \gamma_2 b I_v'(\gamma_2 b) & \gamma_2 b K_v'(\gamma_2 b) & -\kappa_3 b J_v'(\kappa_3 b) & -\kappa_3 b Y_v'(\kappa_3 b) & 0 \\ 0 & 0 & 0 & \kappa_3 c J_v'(\kappa_3 c) & \kappa_3 c Y_v'(\kappa_3 c) & -\gamma_4 c K_v'(\gamma_4 c) \end{vmatrix} = 0, \tag{3}$$

$$(n_4 < n_{eff} < n_3)$$

$$\begin{vmatrix} J_v(\kappa_1 a) & -I_v(\gamma_2 a) & -K_v(\gamma_2 a) & 0 & 0 & 0 \\ 0 & I_v(\gamma_2 b) & K_v(\gamma_2 b) & -I_v(\gamma_3 b) & -K_v(\gamma_3 b) & 0 \\ 0 & 0 & 0 & I_v(\gamma_3 c) & K_v(\gamma_3 c) & -K_v(\gamma_4 c) \\ \kappa_1 a J_v'(\kappa_1 a) & -\gamma_2 a I_v'(\gamma_2 a) & -\gamma_2 a K_v'(\gamma_2 a) & 0 & 0 & 0 \\ 0 & \gamma_2 b I_v'(\gamma_2 b) & \gamma_2 b K_v'(\gamma_2 b) & -\gamma_3 b I_v'(\gamma_3 b) & -\gamma_3 b K_v'(\gamma_3 b) & 0 \\ 0 & 0 & 0 & \gamma_3 c I_v'(\gamma_3 c) & \gamma_3 c K_v'(\gamma_3 c) & -\gamma_4 c K_v'(\gamma_4 c) \end{vmatrix} = 0 \tag{4}$$

$$(n_3 < n_{eff.} < n_1)$$

The J_v, Y_v, I_v and K_v are Bessel and modified Bessel functions of order v respectively. The γ_i and κ_i transversal propagating constants are defined as follows:

$$\gamma_i=\left(\beta_g{}^2-n_i{}^2k_0^2\right)^{\frac{1}{2}}, \kappa_i=\left(n_i^2k_0^2-\beta_g^2\right)^{\frac{1}{2}} \quad (i=1,2,3,4) \tag{5}$$

Also, for easy handling of the problem, the structural parameters are defined as follows.

$$R_1=\frac{n_1-n_3}{n_3-n_2}, R_2=\frac{n_2-n_4}{n_3-n_2}, \Delta=\frac{n_1^2-n_4^2}{2n_4^2}\approx\frac{n_1-n_4}{n_4}, P=\frac{b}{c}, Q=\frac{a}{c} \tag{6}$$

One desired quantity in this investigation is MFD which is related to the field distribution in the fiber through the Equation (7) [13].

$$MFD^2 = 8\frac{\int_0^\infty |\psi(r)|^2 rdr}{\int_0^\infty \left|\frac{d\psi(r)}{dr}\right|^2 rdr}, \quad (7)$$

where, $\psi(r)$ is modal field distribution. The other parameter being studied is A_{eff} of the field distribution which can be calculated through Equation (8).

$$A_{eff} = 2\pi \frac{\left[\int_0^\infty |\psi(r)|^2 rdr\right]^2}{\int_0^\infty |\psi(r)|^4 rdr}. \quad (8)$$

As expressed in the introduction, the main target of this paper is the strain effect study of the MFD and A_{eff} parameters in WII type single mode optical fiber. Getting exposed to strain, the bandgap shift of silica causes the change in the absorption coefficients and affects the refractive index of it. Therefore, the strain-induced bandgap change is related to the changes of the refractive index [14].

The application of force to the fiber in equilibrium causes it to undergo deformation and/or motion. The measure of deformation is labelled strain, ε. Two types of strain exists, normal and shear. Normal strain being the ratio of length change δu, of the stressed element in a direction parallel to the applied force labelled as x is formulated as [15]

$$\varepsilon_i = \frac{\partial u_i}{\partial x_i} \quad (9)$$

Shear strain is a measure of distortion of the stressed element, formulated as

$$\varepsilon_{ij} = \varepsilon_{ji} = \frac{1}{2}\left(\frac{\partial u_i}{\partial x_j} + \frac{\partial u_j}{\partial x_i}\right) \quad (10)$$

A modern multilayer optical fiber response to normal strain, being the chief aim, occurs due to both changes in the refractive index and dimensions of the layer which manage the n_{eff} variation. The term relating the refractive index changing with strain is dominated by photoelastic effect. Physical change in core height and width is related to the Poisson ratio (v). Generally, considering the thermal induced strain due to temperature variation, the change in refractive index as a result of strain can be deduced to be [15]:

$$\Delta n_i = \sum_{i,j=1}^{6} \frac{\partial n_i}{\partial \varepsilon_j}\varepsilon_j + \frac{\partial n_i}{\partial T}\Delta T = -\frac{n_i^3}{2}\sum_{i,j=1}^{6} p_{ij}\varepsilon_j + \frac{\partial n_i}{\partial T}\Delta T, \quad (11)$$

where, p_{ij} are the photoelastic coefficients, n_i is the refractive index of the ith layer, ΔT is the temperature variation and ε_j is the strain tensor element. Assuming the homogeneity and isotropic behavior of silica and also the application of force perpendicular to the fiber cross section, Equation (11) can be simplified to

$$\Delta n_i = -\frac{n_i^3}{2}\left(p_{12} - v\left(p_{11} + p_{12}\right)\right)\varepsilon + \frac{\partial n_i}{\partial T}\Delta T, \quad (12)$$

where, for the pure silica in the wavelength of 1.55μm, p_{11}=0.113, p_{12}=0.252, v=0.17. In analysis of Equation (12), note that among the diverse types of possible strains, the axial type is taken into account which stands for the strain induced to the material when the applied force is perpendicular to the cross section. Strain induction affects the fiber structure in two different concepts: I) Geometrical change of the fiber shape II) Optical change in the fiber. Both the geometrical alteration and optical change result in variation in the effective refractive index of the fiber and thus electrical field distribution. In the Geometrical point of view, the physical changes in width and length of the fiber is related to the Poisson ratio (υ) of the material. However, contribution of this concept in making changes in the fiber behavior and its electrical field distribution is calculated to be negligible comparing to the optical changes and with a high accuracy could be disregarded. In other words, among the optical and geometrical changes induced, the optical variations are totally prevailed and manage the MFD and A_{eff} responses.

Finally, neglecting the refractive index change due to temperature variations, the second term in Equation (12) is dismissed.

3. Simulation results and discussion

Based on the method mentioned in the previous section, the simulation results are illustrated to present the effects of strain on MFD and A_{eff} of the considered WII type optical fiber. It is well known that variation in the structural parameters of the fiber affects the strain impact. Therefore, we study the role of the optical and geometrical parameters in the strain response of the optical fiber. The initial values for structural parameters are as follows:

P=0.7 , Q=0.5 , a=2.5μm , Δ=0.004, R_1 =5 , R_2= -0.6

During the study, the variations made in the parameters' values from their initial points are with respect to the condition approving the single mode feature. In addition, the alterations in the refractive indices of the layers are so that the difference in maximum and minimum values never exceeds 1% and hence the LP approximation is confirmed with high accuracy.

Exploiting Equations (3) and (4) which stand for boundary condition matrixes in WII type optical fiber, the normalized electrical field distribution of the fundamental

mode is simulated for the initial values of the structural parameters at 1.55 µm and exhibited in Figure 2. Referring to the figure, it is apparent that the fundamental electrical field distribution is bell-shaped and peaks in the center corresponding to the highest refractive index, representing the core, of the multilayer structure.

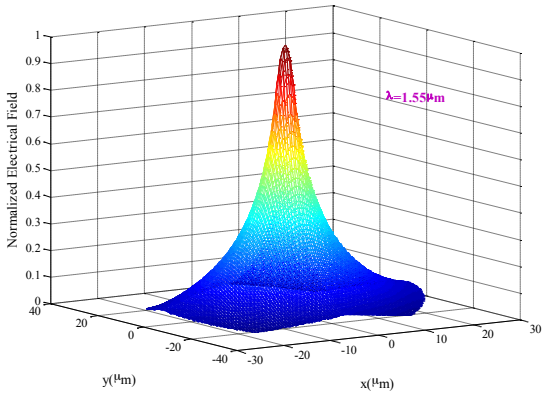

Figure 2. Normalized electrical field distribution in WII type optical fiber with initial structural parameters at 1.55 µm.

In each simulation, all of the parameters are kept constant except the one being examined. An important concept to consider is the obligation to choose the ranges for all the hyper-parameters in a region confirming the single mode feature of the fiber. In order to investigate the strain influence, the range of $\pm 1.2\times10^{-3}$, corresponding to the force of ± 1000 N, has been considered. All the simulations have been accomplished at λ=1.55µm since silica has the smallest natural attenuation at this wavelength. Moreover, in this study the temperature effect has been neglected.

Figure 3 shows the effect of the core radius (*a*) on the mode field diameter variation due to applied strain. Based on the figure, it is obvious that the DC levels of the curves are too large in comparison to their slopes which means that the changes in MFD due to strain is not significant enough to be observed properly. In other respects, the graphs highlight the change in MFD value for different core radius levels and the variation in MFD as a result of strain which determines the curve slopes is approximately lost.

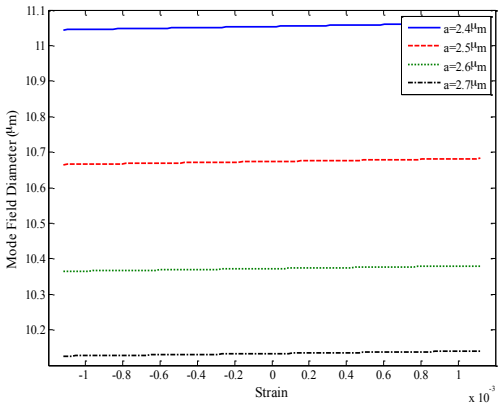

Figure 3. Mode field diameter *vs.* strain for the core radius as parameter.

Hence, for considering the mode field diameter alterations as a result of applied strain, a modification in result representation method is required. To do so, the mode field diameter of the structure is reintroduced through the following relation.

$$\text{Mode field diameter} = \text{MFD} + \text{mfd}(\varepsilon) \quad (13)$$

In Equation (13), MFD is large constant which is calculated in the maximum level of compressive strain and the second term shows the strain dependency of the MFD. For the illustrated case, Mode field diameter as a function of core radius for different values of applied strain is presented in Table 1.

According the presented table, it is evident that the changes due to strain in mode field diameter are not remarkable. In addition, for increasing the core radius value from 2.4 µm to 2.7 µm, the MFD of the fiber corresponding to maximum compressive values are 11.0444 µm, 10.6652 µm, 10.3647 µm, 10.1262 µm. These are the DC levels (MFD constant in Equation (13)) that need to be removed so as to have figures perfectly understandable from strain effect point of view which manages the slopes in the curves.

With the same considerations depicted for the MFD of the fiber, a reintroduction for the effective area is presented through the following relation:

$$\text{Effective area} = A_{eff} + a_{eff}(\varepsilon), \quad (14)$$

where, A_{eff} is the large constant and $a_{eff}(\varepsilon)$ is the strain dependent part of the effective area of the optical fiber. From now on, all of the exhibited figures are for the variable part of the Equation (13) and Equation (14).

Table 1: Mode field diameter value for fiber with different core radiuses corresponding to specific strains at 1.55µm.

	Core radius (µm)	2.4	2.5	2.6	2.7
Mode Field Diameter(µm)	Maximum Compressive strain	11.0444	10.6652	10.3647	10.1262
	No Strain	11.0539	10.6737	10.3724	10.1332
	Maximum Tensile strain	11.0634	10.6822	10.3802	10.1403

3.1. The effects of strain on mode field diameter with variation in optical and geometrical parameters

According to Equation (7) effects of the hyper-parameters in the optical fiber on the mfd(ε) versus strain are independently investigated. Conforming to all the figures exhibited in this subsection, it is obvious that generally mfd(ε) increases gradually as the applied compressive strain diminishes and then changes to the tensile type. In other words, expansion in compressive and tensile strains lead to contrast effects on mfd(ε) and yield reduction and boost, respectively. Through the physical point of view, based on Equation (12), for compressive strain (ε < 0) not only is the refractive index variation due to strain positive but also it has a direct relationship with the layer refractive index value. So, the difference in the core and the first cladding layer refractive indexes grows and thus the light is restricted in the core more than before. This phenomenon generally reduces the mfd(ε). On the other hand, for the tensile strain (ε > 0) the difference in the core and the first cladding layer refractive indexes falls. Hence, the fiber capability to bind the light reduces and the electrical field spreads more in the cladding region. In other respects, the field distribution becomes smoother and consequently the mode field diameter enlarges.

Figure 4 shows the impact of the geometrical parameters on the mfd(ε) variation due to applied strain. The simulation results admit the similar effect of alteration in geometrical parameters of *a* and *Q* on the variation in mfd(ε) as a result of strain. As the numerical amounts allocated to these parameters go up, there is a fall in the curve slopes, and hence the mfd(ε) in the fiber structure is more resistive to strain. In case of the core radius, as this parameter increases while all other optical and geometrical parameters are kept constant, clad takes distance from core which carries the major transition power. Thus, variation in their refractive indexes induce lower impacts on field distribution, and hence reduction in slopes are observed. In contrast, augmentation in the *P* value boosts the slope of the graph. In other words, mfd(ε) exhibits lower sensitivity to strain for smaller passible amounts of *P*. In each figure the exact alterations of the mfd(ε) due to strain for each degree of the hyper-parameters are presented.

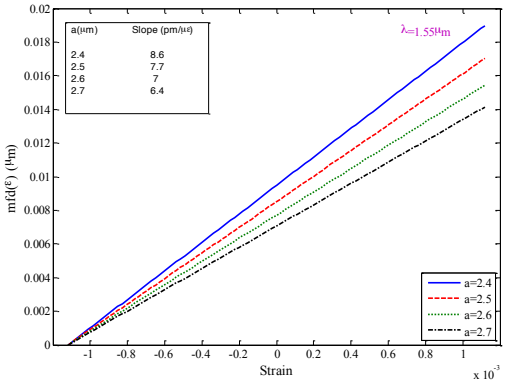

(a)

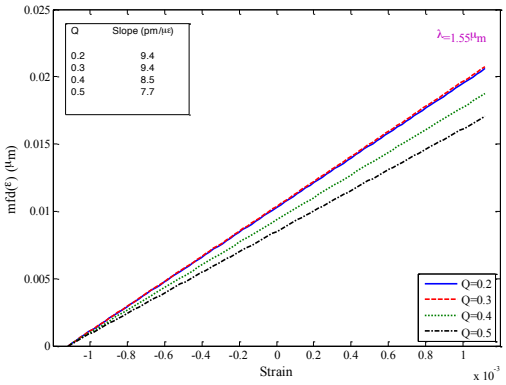

(b)

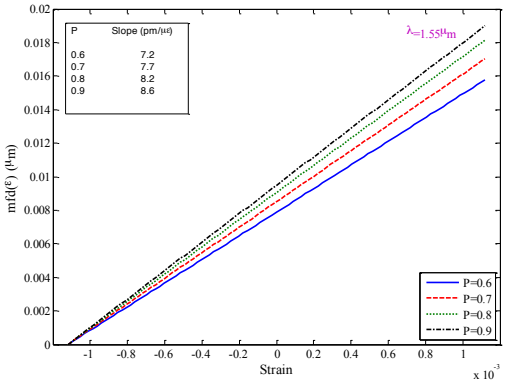

(c)

Figure 4: mfd (*µm*) *vs.* strain for (a) core radius (b) *Q* (c) *P* ,as parameter.

The effect of changes in the optical parameters on the mfd(ε)-Strain graph is demonstrated in Figure 5. According to the figure, generally growth in of all the optical parameters lead to the reduction in the strain

sensitivity of the mfd(ε) of the fiber structure. The alterations made to the curve slopes due to changes in Δ are substantial. The growth in Δ is corresponding to increment in core refractive index which leads to the restriction of light in the core more than before. In this situation the impression of the cladding layers on the field distribution is limited. Therefore, the change in the refractive indexes in the cladding layers as due to strain induction leads to inconspicuous variation in mfd(ε) response which is illustrated by decline in curve slopes. Higher viable amounts of Δ are preferred in case the lower variation in the mfd(ε) due to strain is desirable. However, as demonstrated by Figure 5 (b), all of the curves carry almost the same slope with regards to R_1. For confirmation of this outcome, it is advantageous to pay attention to the structural changes in the fiber as a result of extension in R_1 value. Based on the Equation (3), as R_1 goes up both n_2 and n_3 fall minimally. On the other hand, according to Equation (8), the variations in n_2 and n_3 due to strain reduce. Conclusively, the changes in R_1 will not affect the slope of the curves remarkably. Figure 5 (c) refers to the R_2 effect on mfd(ε) variation due to strain. According to this figure, magnification in R_2 amplitude results in minimal growth in graph slope. As an overall, the mfd(ε) response to strain is resistant to changes in R_1 and R_2 and does not exhibit considerable alteration with variation in these optical parameters.

To sum up the results extracted in this subsection, it is obvious that the mfd(ε) absolutely increases as the tensile strain goes up. On the other hand, increment in the amplitude of the compressive strain results in reduction of the mfd(ε). Moreover, analyzing the outcomes of the figures, it can be claimed that Δ is the parameter having substantial impact on the mfd(ε)-Strain curve. Nonetheless, consequence of tiny deviation in determination of Δ is remarkable change in the resistivity of the mode field diameter of fiber structure to applied strain. If aimed to employ a WII type fiber having mode field diameter with the least sensitivity to strain, whether compressive or tensile, for the most desirable performance, Δ should be as large as possible. On the other hand, the strain response is approximately insensitive to changes in R_1 and R_2, and thus manufacturing error in determination of R_1 and R_2 is not highly problematic.

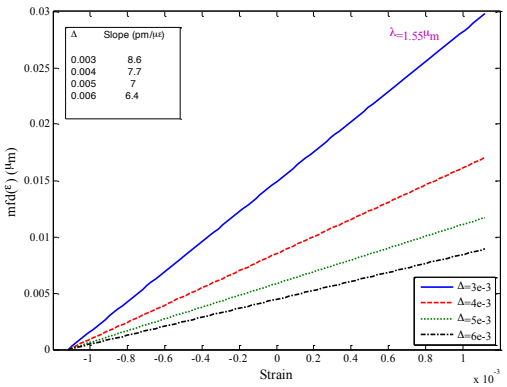

(a)

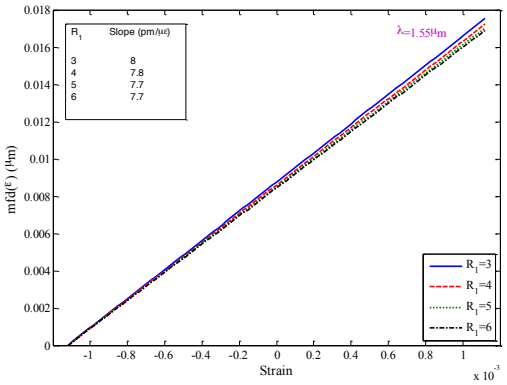

(b)

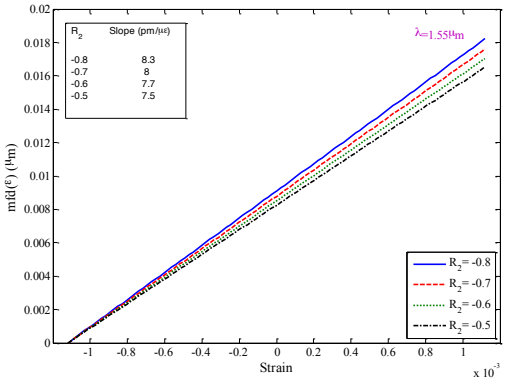

(c)

Figure 5: mfd (μm) *vs.* strain for (a) Δ (b) R_1 (c) R_2 ,as parameter.

3.2. The effects of strain on effective area with variation in optical and geometrical parameters

According to the Equation (8), effects of the hyper-parameters in the optical fiber on the $a_{eff}(\varepsilon)$ due to strain are investigated independently. Following the same explanations in previous subsection about mfd(ε), a brief look at all the figures presented in this subsection admits that there is a rise in $a_{eff}(\varepsilon)$ as the applied strain varies moderately from -1.2×10^{-3} to $+1.2\times10^{-3}$. In order to study the sensitivity of effective area of the WII type optical

fiber to strain for different values of structural parameters, the second term of the Equation (12) is simulated.

Figure 6 demonstrates the impression of geometrical parameters on $a_{eff}(\varepsilon)$ versus strain in modern multilayer WII type fiber optic.

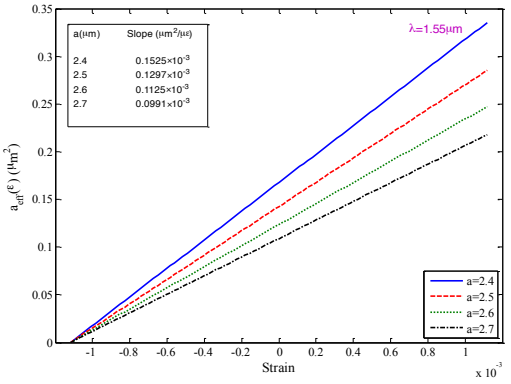

(a)

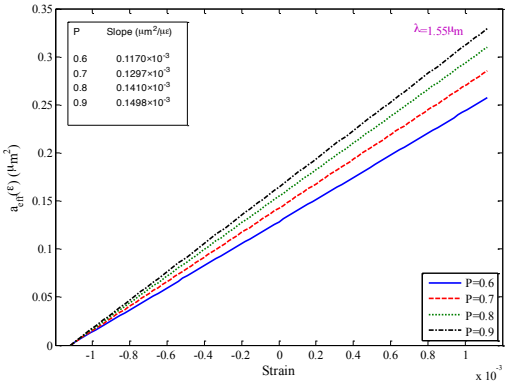

(b)

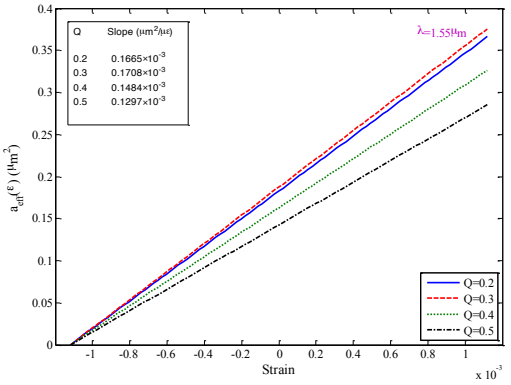

(c)

Figure 6: a_{eff} (μm^2) *vs.* strain for (a) core radius (b) P (c) Q ,as parameter.

The core radius influence on $a_{eff}(\varepsilon)$ versus strain curve is demonstrated in Figure 6 (a). According to this figure, $a_{eff}(\varepsilon)$ variation due to strain has an apparent opposite relationship with core radius changes. It indicates that preference of lower amounts for a leads to more changes in $a_{eff}(\varepsilon)$ -Strain graph slope. However, the effect of P on $a_{eff}(\varepsilon)$ alterations as a function of strain is inverse as presented in Figure 6 (b). Small values for P makes the variations in $a_{eff}(\varepsilon)$ lower while the greater amounts of P augments it. The impact of Q on changes in $a_{eff}(\varepsilon)$ due to strain is represented in Figure 6 (c). This case is of complexity which can be explained by focusing on Q effect on the structure of the multilayer WII fiber presented in Figure 1. With increment in the Q value, both n_2 and n_3 layers narrow. Nevertheless, this occur for n_2 with a higher pace in a way that increasing the Q from 0.2 to 0.3 results in almost 50% reduction in n_2 width. It makes the role of n_3 layer in modal field distribution more considerable due to reduction of the distance to the core. Therefore, getting more sensitive to n_3 variations, the alterations in $a_{eff}(\varepsilon)$ changes due to strain augment. However, with further increments in Q value, the fall in the width of n_2 and n_3 layers cause the reduction of the influences of these layers. In this circumstances, the $a_{eff}(\varepsilon)$ variation in simplified structure shows lower sensitivity to strain changes.

The impact of optical parameters on the $a_{eff}(\varepsilon)$-strain graph is studied in Figure 7. Figure 7 (a) illustrates the effect of Δ on the graph of $a_{eff}(\varepsilon)$ versus strain. Based on the simulation results for Δ variation, it is evident that the consequence of increment in Δ value is the significant descend in $a_{eff}(\varepsilon)$ variation due to strain. Figure 7 (b) demonstrates the variation of $a_{eff}(\varepsilon)$ versus strain while the hyperparameter being studied is R_1. The insignificant changes in slopes for different amounts of R_1 are apparent. This feature is explainable just same as the way presented in previous subsection. However, for smaller amounts of R_1 higher variations in $a_{eff}(\varepsilon)$-Strain graph are attained. The R_2 impact on $a_{eff}(\varepsilon)$ alterations due to strain is shown in Figure 7 (c). Although the changes in slope for different values of R_2 are not remarkable, as an overall trend the $a_{eff}(\varepsilon)$ variation increases as the amplitude in R_2 boosts.

In conclusion, based on the figures illustrated in this subsection, analogues to the previous subsection, it is the Δ which has the most considerable influence on $a_{eff}(\varepsilon)$ variation as a function of Strain. Logically, full attention in determination of Δ is essential. The highest possible amount for Δ is preferred in case it is desired to have a structure with the effective area merely resistive to strain while the single mode feature of the fiber is maintained, either. However, R_1 has the least impact and the fiber is almost insensitive to changes in R_1 and extra concentration on this parameter is not necessary.

Larger effective areas are generally associated with larger mode field diameters which, in turn, imply higher bending losses. A quality factor, defined as the ratio of effective area over the square of mode field diameter, is introduced as a means of assessing and comparing the overall performance of different large effective area fibers

[3]. This factor is a dimensionless quantity that can be used to determine the trade-off between mode field diameter and effective area.

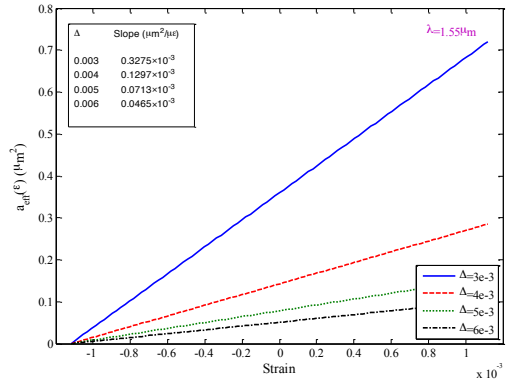

(a)

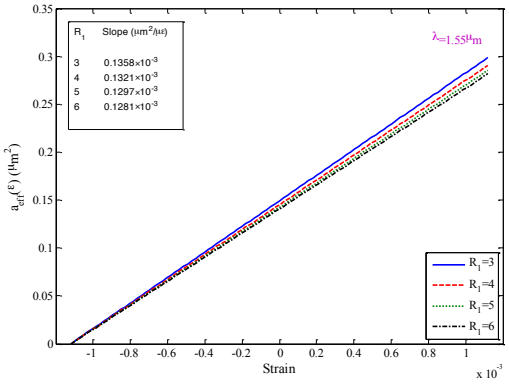

(b)

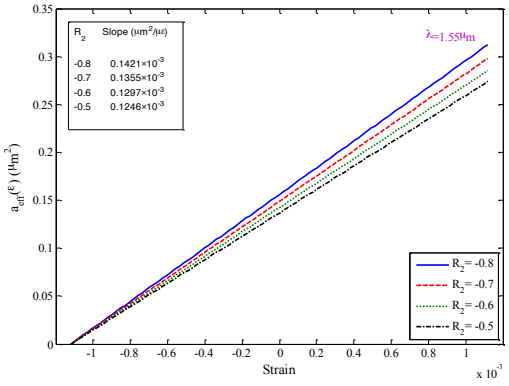

(c)

Figure 7: a_{eff} (μm^2) *vs.* strain for (a) Δ(b) R_1 (c) R_2 ,as parameter.

Based on the results exhibited in 3.1 and 3.2 subsections, taking the changing manner of structural parameters into attention, the disparity in the selected intervals and thus the step of variation for each parameter is obvious which is as a result of endeavor in maintaining the single mode property and holding the LP approximation. Furthermore, it is evident that application of tensile strain results in rise in both mode field diameter and effective area. On the other hand, when the fiber is exposed to compressive strain, the two transition parameters of mode field diameter and effective area fall in amplitude. However, effective area faces a higher variation due to strain in comparison to the mode field diameter alteration for the identical strain amount. Considering the definition of the quality factor (Q_f), which stands for the fiber performance quality, it is claimed that increment in tensile strain induced to the fiber modifies the quality factor. Conversely, in case the fiber is in a situation experiencing compressive strain, the quality factor of the fiber is reduced. Figure 8 demonstrates the quality factor behavior in WII type single mode optical fiber holding the initial values for optical and geometrical parameters mentioned in the first paragraph of section 3 as a function of strain at the wavelength of 1.55μm.

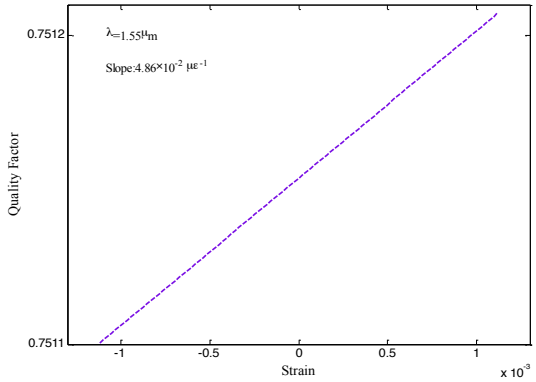

Figure 8: Quality factor as a function of strain for the fiber with initial structural parameters.

According to the data presented in the figure, the quality factor variation due to strain is calculated to be 4.86×10^{-2} $\mu\varepsilon^{-1}$. In other words, for lower compressive strains the variation in quality factor is not critical but higher amounts of compressive strain can negatively affect the fiber performance. Note that the quality factor is smaller than unity in the inner depressed clad fibers (W structures) [3].

In order for studying the effect of axial strain as an external perturbations on transition parameters of the optical fiber, the strain response is investigated in this article. Admittedly, implementation of the experimental trail so as to validate the acquired results is on demand. However, due to a lack of essential laboratory facilities, the research is restrained in simulation stage. Yet, the sequence is a mature proposal for further experimental researches in any facilitated laboratory as this fiber structure with its sensitivity to strain application, also exhibits the potential for employment is sensing domains, either.

4. Conclusion

The variation in the mode field diameter and the effective area of the single mode WII type optical fiber due to strain is studied in this paper. The simulation results indicate that both the mode field diameter and effective area boost as tensile strain grows and the amplitude of the compressive strain diminishes. However, due to higher variation in effective area in comparison to mode field diameter, the quality factor of the fiber is raised slightly with the rate of 4.86×10^{-2} $\mu\varepsilon^{-1}$. Furthermore, among the transmission parameters, the variation in mfd(ε) and $a_{eff}(\varepsilon)$ due to strain is approximately insensitive to R_1 and has the highest dependence on Δ. In higher amounts of Δ, due to the specific structure of the WII type fiber, the effect of cladding layers on the field distribution of fundamental mode is decreased which leads to the fall in the graph slopes of mfd(ε) and $a_{eff}(\varepsilon)$ strain responses. Therefore, in manufacturing stage, the least error in Δ value determination must be accomplished.

5. References

[1] S. Makouei, M. S. Oskouei, A. Rostami, Study of bending loss and mode field diameter in depressed inner core triple clad single-mode optical fibers, *Optics Communications* 280: 58-67, 2007.

[2] O. Celikel, Mode field diameter and cut-off wavelength measurements of single mode optical fiber standards used in OTDR calibrations, *Optics and Quantum Electronics* 37: 587-604, 2005.

[3] M. S. Oskouei, S. Makouei, A. Rostami, Z. D. Koozeh Kanani, Proposal for optical fiber designs with ultrahigh effective area and small bending loss applicable to long haul communications, *Applied Optics* 46: 6330-6339, 2007.

[4] Y. Namihira, Relationship between nonlinear effective area and mode-diameter for dispersion shifted fiber, *Electronics Letter* 30: 262–264, 1994.

[5] J. Cozens, A. Boucouvalas, Coaxial optical couplers, *Electronics Letters* 18: 138-140, 1982.

[6] Y. Hussey, C. Li, T. Briks, Triple-clad single-mode fibers for dispersion shifting, *J. Lightwave Technology* 11: 1812-1819, 1993.

[7] X. Zhang, X. Wang, The study of chromatic dispersion and chromatic dispersion slope of WI- and WII-type triple-clad single-mode fibers, *Optics & Laser Technology* 37: 167-172, 2005.

[8] H. Hattori, A. Safaai-Jazi, Fiber designs with significantly reduced nonlinearity for very long distance transmission, *Applied Optics* 37: 3190-3197, 1998.

[9] A. Rostami, S. Makouei, TEPMERATURE DEPENDENCE ANALYSIS OF THE CHROMATIC DISPERSION IN WII-TYPE ZERO-DISPERSION SHIFTED FIBER (ZDSF), *Progress in Electromagnetic Research B* 7**:** 209-222, 2008.

[10] A. Rostami, M. S. Oskouei, Investigation of Chromatic Dispersion and Pulse Broadening Factor of Two New Multi-clad Optical Fibers, *Int. J. Computer Science and Network Security* 6: 60-68, 2006.

[11] A. Rostami, M. S. Oskouei, Investigation of dispersion characteristic in MI- and MII-type single mode optical fibers, *Optics Communications* 271: 413-420, 2007.

[12] X. Tian, X. Zhang, Dispersion-flattened designs of the large effective-area single-mode fibers with ring index profiles, *Optics Communications* 230: 105-113, 2004.

[13] A. Gatak, K. Thyagarajan, *Introduction to fiber optics,* 3rd ed.; Cambridge university press, 2002

[14] J. Cai, Y. Ishikawa, K. Wada, Strain induced bandgap and refractive index variation of silicon, *Opt*ics *Express* 21: 7162-7170, 2013.

[15] J. Castrellon-Uribe, Fiber Optic Sensors. In *Optical Fiber Sensors: An Overview*; Yasin, Moh., Ed.; InTech, pp. 112-139, 2012.